Spectrum-Sharing Method for Co-Existence Between 5G OFDM-Based System and Fixed Service

WALID A. HASSAN[1,2], **(Senior Member, IEEE), HAN-SHIN JO**[3], **(Member, IEEE),**
SALAMA IKKI[1] **(Senior Member, IEEE), AND MAZIAR NEKOVEE**[4,5], **(Member, IEEE)**

[1]Electrical Engineering Department, Faculty of Engineering, Lakehead University, Thunder Bay, ON P7B 5E1, Canada
[2]Basrah Wireless Communication Research Laboratory, Information and Communication Engineering Department, Basrah University College of Science and Technology, Basrah 24001, Iraq
[3]Department of Electronics and Control Engineering, Hanbat National University, Daejeon 34158, South Korea
[4]Department of Engineering and Design, Sussex University, Richmond 2C08, U.K.
[5]Quantrom Technologies LTD Whitefriars, Lewins Mead, Bristol, BS1 2NT, U.K.

Corresponding author: Han-Shin Jo (hsjo@hanbat.ac.kr)

ABSTRACT This study investigates the co-existence of fifth generation (5G) mobile communication systems and fixed service (FS) in the 28-GHz band through the utilization and modification of an existing spectrum-sharing method known as the advanced minimum coupling loss (A-MCL) model. The proposed model is based on the power spectral density (PSD) overlap between the 5G orthogonal frequency-division multiplexing (OFDM)-based system and the FS. Spectrum-sharing studies typically need 5G parameters, such as the spectrum emission mask (SEM); however, no such information is available for the new system to achieve accurate results. The proposed model is suitable for spectrum-sharing studies between 5G and other wireless systems without the need for the 5G SEM. Moreover, the existing model is implemented in a new application (i.e., 5G) in the 28-GHz band with different 5G bandwidths. Furthermore, the FS parameters and its frequency allocation are selected based on the Canadian standards to obtain preliminary results for the co-existence between the 5G system and the FS. Results show that co-existence is feasible when certain distances are applied, especially with higher 5G bandwidths (such as 0.5 and 1 GHz) when the 5G system acts as an interferer. In addition, the antenna position plays a major role in reducing the required separation distances between the victim receiver and the interfering transmitter. This model can be used for any future mobile generation such as the sixth generation (6G) mobile system if its PSD is known. This study is concurrent with the worldwide spectrum-sharing studies requested by the International Telecommunication Union for WRC-19.

INDEX TERMS 5G, advanced minimum coupling loss, co-existence, fixed service, interference, power spectral density, spectrum-sharing

I. INTRODUCTION

With the introduction of any new wireless communication system, spectrum allocation is one of the main challenges that such system faces. This is the case with the introduction of the Fifth Generation (5G) mobile communication system, also known as the International Mobile Telecommunication-2020 (IMT-2020) system [1]. The 5G

The associate editor coordinating the review of this manuscript and approving it for publication was Wenjie Feng.

system was officially announced at the last World Radio Conference in 2015 (WRC-15) in Geneva [2]. At WRC-15, where two main outcomes were announced to prepare for 5G system operation; first, a new spectrum was allocated for mobile services in the millimeter-wave (mmWave) band between the 24 GHz and 86 GHz bands. Second, spectrum-sharing studies in these candidate bands were called for by the International Telecommunication Union (ITU). The output of these studies is one of the agenda items at WRC-19 [2].

Early spectrum-sharing studies have faced a major challenge regarding the lack of parameter information related to the new system. These studies incorporate inaccurate results because they are conducted before the launch of the new system and the system important co-existence parameters such as the Spectrum Emission Mask (SEM) of the new system, its transmitted power and the network deployment is not yet identified. In this case, analytical and statistical models are used, including the Minimum Coupling Loss (MCL) model and Monte Carlo methods [3]. The lack of SEM information is the main limitation of these methods. To overcome this limitation, studies [4]–[10] have included the overlap of the Power Spectral Densities (PSDs) of the new system as an interferer and the victim receiver to overcome the unavailability of the SEM of the new system.

The MCL model was first published in [3] and was used in the European Conference of Postal and Telecommunications (CEPT) spectrum-sharing studies. This study also presents an Enhanced MCL (E-MCL) model and Monte Carlo method. They were used in cellular systems such as the 2nd and 3rd mobile generation (2G and 3G, respectively) systems [3]. The MCL method was further enhanced to the Advanced MCL (A-MCL) in order to be suitable for assessing the compatibility between the 4th mobile generation (4G) system and other systems [4], [5], [8], [10]. These studies utilize the A-MCL method to investigate the co-existence between the Orthogonal Frequency-Division Multiplexing (OFDM)-based system (i.e., 4G) and a Fixed Service (FS). Other studies utilized this method to determine the feasibility of co-existence between the 4G and FM systems [6], [9].

In this paper, a case study is presented to investigates the co-existence between the 5G system and the FS in the 28 GHz band based on modifications and simplifications to the existing A-MCL model. The 28 GHz band was selected because it is considered a favorable 5G band, especially in the US, Korea, and Japan [11]. Canada is expected to follow the US 5G spectrum allocation. The frequency allocations and some of the main FS parameters are based on Canadian frequency allocations and Canadian standards. The co-channel sharing scenario is investigated in urban microcell (UMi) environments. Rural macrocell (RMa) environments were not included since the RMa network requires large coverage and operates at centimeter-wave (cmWave) frequencies (i.e., below 6 GHz) [12].

The three main contributions of this study are as follows. First, the A-MCL model is used in a new application, (the 5G system), based on the fact that it will be the first time a cellular service will operate in the mmWave band. The current method is modified by adding a composite three-dimensional (3D) beamforming antenna to the 5G system. Second, a more simplified derivation of the PSD overlap is presented and compared to those in previous studies [4]–[10.]. Third, unlike the studies in [4]–[10] that modeled only one way of interference (i.e. computing the PSD overlapping interference from FS into the mobile service), this study computes and models the PSD overlapping in both ways of interference between the mobile service and FS. This model is greatly effective when a spectrum-sharing study is needed due to the lack of availability of the new system co-existence parameters. This model is suitable for any spectrum-sharing study that needs to investigate spectrum-sharing with existing services without the need for the SEM. Moreover, the model can be modified with the introduction of any new wireless system based on the PSD overlap and hence can be used for the 6th or even the *n*th mobile generation as long as the mathematical model of the respective PSD is known.

The rest of this paper is organized as follows. Section II reviews the 5G and FS status in Canada, while also analyzing the 28 GHz status in Canada. Section III presents related studies that utilize the A-MCL model and the latest studies on the co-existence between the 5G and FS systems. In Section IV, the A-MCL model is presented first along with its derivation followed by the suggested simplifications and modifications to the existing A-MCL model. In addition, the system parameters are presented. The results for spectrum-sharing between the FS and the 5G system are discussed and analyzed in Section V. Finally, Section VI concludes this study.

II. 5G AND FS IN CANADA
A. MMWAVE CANDIDATE BANDS FOR 5G DEPLOYMENT
At WRC-15, the cellular mobile services bands were divided into three categories: low-range (between 0.6 and 3 GHz), midrange (between 3 and 6 GHz), and high-range (between 20 and 80 GHz) [11]. The low-range and midrange frequency bands are already allocated for the usage of mobile service such as 2G, 3G, 4G and can be used by the 5G system, especially for rural deployment. With the introduction of 5G, the higher bands will be used for the first time for mobile services. Each of these bands has its own signal propagation characteristics. For instance, the low-range band has the benefits of a longer wavelength that has the ability for penetration and provides a wider coverage with a lack of providing high data rate capacity. However, the high-range band is the opposite and is meant for applications with a high capacity that can be used and a shorter range. The midrange band is the optimum solution for urban coverage balancing both coverage and capacity [1], [11], [13]. Table 1 lists the 11 candidate bands for the 5G system proposed at WRC-15 between the 24 GHz and 86 GHz bands. In addition, the 28 GHz band was proposed by the US, Japan, and Korea to be allocated for the 5G system [11].

B. 5G SPECTRUM IN CANADA
The Canadian spectrum regulator known as Innovation, Science and Economic Development (ISED) released a consultation document regarding the allocation of 28 GHz, 37-40 GHz, and 64-71 GHz for the deployment of the 5G system [14] in June 2017. This was followed by another amendment to this document on releasing 26.5-27.5 GHz to support the 5G system in June 2018. In these consultations, suggestions and questions had been set for public regarding

TABLE 1. IMT-2020 candidate bands [2].

	mmWave frequencies (GHz)	Available Bandwidth (MHz)	General Remarks
1.	24.25–27.5	3.25	Resolution 238 [2] set these bands to the mobile service on a primary basis.
2.	37–40.5	3.5	
3.	42.5–43.5	1	
4.	45.5–47	1.5	
5.	47.2–50.2	3	
6.	50.4–52.6	2.2	
7.	66–76	10	
8	81–86	7	
9.	31.8–33.4	1.6	Resolution 238 [2] considers these bands to require additional allocation to the mobile service on a primary basis (i.e., monglobal mobile allocation).
10	40.5–42.5	2	
11.	47–47.2	0.2	
12	27.5 –28.5	1	Not included in the ITU 5G bands but suggested by the FCC.

spectrum policies, restrictions, and sharing studies in the mentioned bands. A decision will be made after receiving feedback, and ISED will consult further [14]. The feedback for the consultation and the amendment were received in October 2017 and July 2018 [15].

Documents were received from various analysis and research agencies that include 5G America, the Dynamic Spectrum Alliance (DSA), the Global Mobile Supplier Association (GSMA), the Wifi Alliance, and the Radio Advisory Board of Canada (RABC). Mobile and wireless communication industries also contributed to the feedback, such as Bell Mobility; the IEEE LAN/Man Standard committee; Intel Corporation; Microsoft; Nokia; Ericsson Canada; Huawei Technologies Canada; Samsung Electronics Canada, Inc.; Sikli Communication; Rogers Communications; Sasktel; Starry, Inc.; Shaw Communication, Inc.; Telus; and GOGECO Communication, Inc. Even Facebook, Inc. submitted their feedback in support of their high-altitude platforms (HAPs) for internet service distribution to rural areas.

Moreover, the satellite companies gave their feedback and concerns regarding their current and future operation of Fixed Satellite Service (FSS). These companies include Intelsat; Ciel; Telesat Canada; TeraGo; ViaSat; Xplornet Communication, Inc.; Space X; and Canada, Inc. Finally, comments were also received from health organizations concerned with the emissions of the 5G system, which can be found in [15]. It is expected that on the basis of this feedback, the Canadian frequency spectrum regulator will announce its 5G spectrum in the coming months of 2019. An auction for the 5G system in Canada is expected in 2020 [16]. At the time of writing this paper, no decision had yet been made regarding the 26.5-27.5 GHz, 28 GHz, 37-30.80 GHz, and 64-71-GHz bands [15]. Nothing related to the spectrum-sharing between the FS and the 5G system was discussed in the
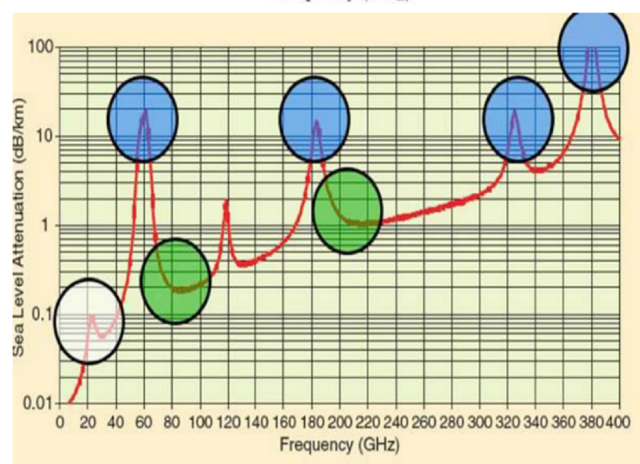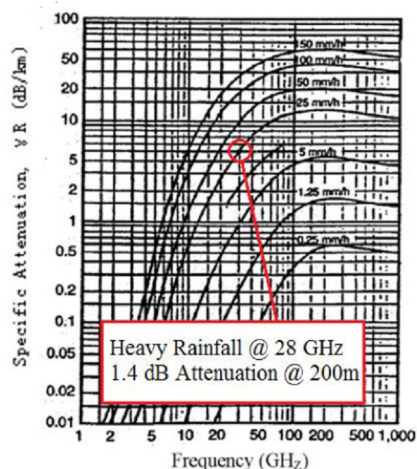
Canadian spectrum regulatory consultation, amendment and feedback [14], [15].

Other issues such as licensing, changing band plans, suggesting policies, and co-existence with the FSS were discussed, which is beyond the scope of this paper. [14], [15].

1) 28 GHZ BAND

The 28 GHz band has received a considerable amount of interest from the Federal Communication Commission (FFC) in the US, Japan, and Korea [11]. What really makes the 28 GHz band more favorable than other bands is that includes radio propagation characteristics and its frequency allocation as primary service in the 28 GHz band. The first work that suggested the allocation of the 28 GHz band to 5G services was presented in [17] in 2013. The authors also discussed the main concerns regarding the signal attenuation in the higher frequency when used for cellular services. The attenuation can be due to rainfall and or due to atmospheric absorption. It is expected that the cell radius in urban areas for 5G will be in the range of 200 m [17]. This fact can overcome the attenuation issues due to atmosphere and rainfall, as can be seen in Fig. 1.
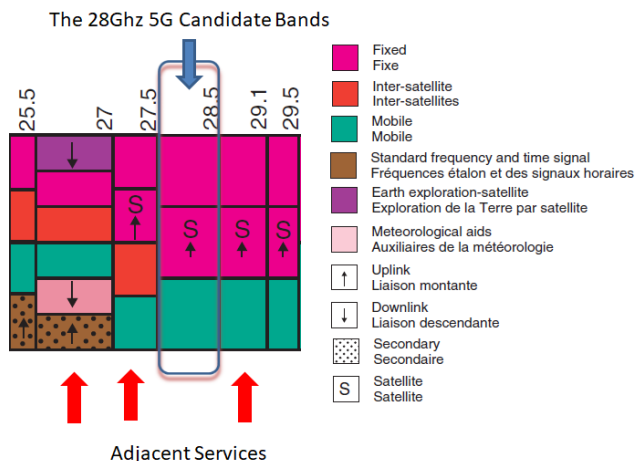
The upper figure of Fig. 1 depicts the relationship between the rate of rainfall and the operating frequency, whereas the bottom figure shows the relation between the attenuation level verse the operating frequency. In Fig. 1 (top) it can be seen that the attenuation is 0.6 dB at the 28 GHz band with a rainfall rate of 7.6 mm/h for a cell radius of 200 m [18]. Even with heavy rainfall rate of 25mm/h, the attenuation is 1.4 dB for the same cell radius. In Fig. 1 (bottom), the 28GHz band had the lowest atmospheric absorption in the frequency range 20 GHz to 400 GHz. The figure shows that the attenuation level is 0.012 dB at the 28 GHz. These facts hence show that the attenuation due to rainfall and atmosphere does not create

FIGURE 1. (Top)Rain Attention in dB/km verse frequency range from 1-1000 GHz [17]. (Bottom) Atmosphere attenuation in dB/km verses frequency range (0-400 GHz) [18].

FIGURE 2. 28 GHz band based on Canadian frequency allocation [55].

Moreover, the EESS is the primary service in the 25.5-27 GHz band in all regions [19]. These issues make the spectrum-sharing with mobile service more complex. This shows that the 28 GHz band have less spectrum-sharing constrain compared to the 26 GHz band which makes it more favorable. Since Canada is in ITU Region 2, it is expected that Canada will follow the FCC path for 5G deployment. The ITU Region 2 historically is harmonized in spectrum allocation and led by the FCC [11], but nothing has been officially released by the Canadian spectrum regulator regarding the assignment of this band to the 5G system [15]. The current spectrum allocation in Canada for the 28 GHz band is presented in Fig. 2 and Table 2 present.

TABLE 2. Service in the 28 GHz band [2].

5G Candidate Band (GHz)	Canadian Allocation (GHz)	Primary Services	Secondary Services
27.5–28.5	27.5–28.5	FS	N/A
		FSS (UL)	
		Mobile	

Table 2 and Fig. 2 indicate that the FS system is the major system that will affect or will be affected by the deployment of the 5G system in these band, especially since it is the primary service in the 28 GHz band. It is observed that 1 GHz will be available for the 5G system (i.e., 27.5-28.5 GHz). The FSS uplink is also a major issue, as it will produce high power for the satellite station, which is another research topic to investigate more deeply. Similarly, Table 3 indicates that the FS is one of the primary services in the bands below and above the 28 GHz band that will be affected by or affects the 5G system. In addition, the Earth Explorer Satellite Service (EESS) system is another service that may cause interference in this band since its has a downlink transmission. The study in [20] suggests a distance of less than 1 km for protection in order for both systems to share spectrum, but more studies are needed to confirm these findings.

additional path loss to the 28GHz signal when used for 5G services [17].

The ITU divides the world into three regions, Region 1 which includes Europe, Africa and parts of Asia such as Iraq and the Gulf countries up to the Iranian borders at the west [19]. Region 2 includes both North and South America and some parts of Oceania. Finally, Region 3 begins from the Iranian borders at the east and includes Asian countries (excluding the Asian counties that are part of Region 1) and most parts of Oceania [19]. Based on the ITU spectrum allocation, the 28 GHz (i.e. from 27.5 GHz till 28.5 GHz) band had only three services (i.e. FS, FSS and Mobile) in it with the priority giving to the FS services. This allocation is applied to the three ITU regions [19]. However, the 26 GHz band (i.e. 24.25-27.5) consists of five sub-bands in the three ITU regions and there are nine services within these sub-bands (i.e. FS, FSS, Mobile, EESS, Inter-Satellite, Radionavigation, Radiolocation Satellite, Standard frequency and time signal-satellite, Space Research) [19]. In these sub-bands there are some vital services that are operating as a primary service. For example, the FSS is the only service operates in the sub-band 24.65-24.75 GHz.

TABLE 3. Service below and above the 28 GHz band [2].

Service Below the 28 GHz Band			Service Above the 28 GHz Band		
Canadian Allocation (GHz)	Primary Services	Secondary Services	Canadian Allocation (GHz)	Primary Services	Secondary Services
25.5–27	EESS (DL)	SFTSS (UL))	28.5–29.1	FS	N/A
	FS			FSS (UL)	
	IS			M	
	M				
	SR				
27–27.5	FS	N/A	29.1–29.5	FSS (UL)	N/A
	FSS (UL)			M	
	IS				
	M				

TABLE 4. Comparison between the lte and verizon 5G systems [22].

PHY parameter	LTE (Rel. 8-14)	Verizon 5G
Downlink	OFDM	OFDM
Uplink	(SC-FDMA)	OFDM
Subcarrier spacing (kHz)	15	75
Sampling rate (MHz)	30.72	153.6
Bandwidth (MHz)	20 MHz	100 MHz
No. of Carriers	2048	2048
Multiplexing	FDD/TDD	Dynamic TDD
Max. Resource Blocks	6, 15, 25, 50, 75, 100	100

C. FS IN THE 28 GHZ BAND IN CANADA

The spectrum from 3 GHz to 30 GHz is shared between the FS and the FSS [14]. The sharing is based on a soft portioning concept, which permits the two services to utilize the spectrum but with priority given to one in various cases [14]. The 28 GHz band is allocated for the FS, mobile, and FSS on a coprimary basis. The FS is currently given priority over the FSS in this band [14]. The services that are deployed are the local multipoint communication services (LMCSs). The technical specifications of the deployment of the FS in Canada can be found in [21].

D. 5G OFDM-BASED SYSTEM

OFDM remains a vital waveform candidate for the 5G system because of its success in 4G and Long-Term Evolution Advanced [22]–[27]. In addition, the 5G system will be diverse and will use OFDM as one of its waveforms [22], [23]. New waveform candidates are still in the development phase and have not been officially released as mobile cellular waveforms. In addition, most 5G trials and 5G prototypes are OFDM-based, as stated in [23] and [28]. For example, the specifications of the Verizon 5G system are listed in Table 4 [22]. Furthermore, 3GPP version 38 relies on OFDM as a specification [29] as 5G waveform candidate. On the basis of the aforementioned arguments, this study assumes that 5G is an OFDM-based system for this sharing study in the 28 GHz band.

III. RELATED STUDIES

A. STUDIES RELATED TO THE MCL AND A-MCL METHODS

As mentioned in Section I, the MCL, E-MCL, and Monte Carlo methods were first introduced in [3] and were developed by the CEPT to determine a unified method

for evaluating the minimum frequency/distance separation between two systems that share a frequency band. Each of these methods had its respective advantages and disadvantages; the MCL method is suitable for finding the co-existence results for the worst-case scenario. It is simple and does not require a complex calculation that needs a computer. One of the main disadvantages is that the results are considered spectrally inefficient because of the large guard band. In addition, the separation distances are extremely large when the free-space propagation model is used. The SEM of the interferer is needed in the calculations.

The Monte Carlo method requires all of the details of the victim and interfering systems along with the environmental details. The results are in terms of the probability of interference. This requires a complex calculation that needs a computer to simulate it. It can be used for large systems such as Code-Division Multiple Access (CDMA)- and Orthogonal Frequency-Division Multiple Access (OFDMA)-based systems. The results are considered to be spectrally efficient, but they rely significantly on the input parameters of the victim, interferer, and sharing scenario, which making this method inappropriate to use when introducing a new system. The E-MCL method is the middle method between the MCL and Monte Carlo methods. The pathloss includes the fading of the desired signal of the victim system. Moreover, the power control can be included.

The studies in [4], [5], [10], and [30] present a new analytical method that improves the MCL method, known as the A-MCL method, for the analysis of an OFDM-based IMT-A system and the FS in the 3.4-5-GHz band. The A-MCL method extends the ability of the MCL method to be suitable for 4G system spectrum-sharing with other services with less information about its parameters at the time of those studies. This method overcomes the limitations of the conventional MCL method in finding the co-existence between two systems without the need for the SEM of the interfering system. Other uses of the A-MCL method in [6], [7], and [9] consider analogue broadcasting to be a victim in the 800 MHz band.

In order to use the A-MCL method for the 5G system, some modifications and additions to the A-MCL method are needed so that it is suitable for the 5G system. In addition, since the 5G system will operate in the mmWave bands,

the method needs to address this. These details are presented in Section IV.

B. CURRENT STUDIES FOR THE SPECTRUM-SHARING BETWEEN THE FS AND 5G SERVICES

In this subsection, the latest studies on spectrum-sharing between the 5G and FS systems are presented. In [31], the co-existence between the 5G system and a point-to-point FS station in the 70 GHz and 80 GHz bands is addressed. This study is based on the existing geometry of the FS station. It utilizes the actual data of buildings from a database to compute the interference by 5G users on the FS. The results indicate that the interference level is below the noise floor owing to the high loss attenuation in the 70 GHz and 80 GHz bands.

In [32], the co-channel interference in the 28 GHz and 70 GHz bands were extensively investigated. This study shows that the FS and FSS are the systems that will share these bands with the 5G system as a victim system. The findings equally show that there is a potential of interference at the FS station from the 5G system in the 28 GHz band. The interference assessment to and from the FS from the 5G system in the 15 GHz band was explored in [33]. The results indicate that the co-channel interference is above the required interference criteria for the FS. In contrasting fashion, the interference from the FS system is acceptable for the 5G downlink system (i.e., 5G user equipment (UE)). In [34], a numerical simulation was conducted to study the co-existence between the 5G system and the FS in the 28 GHz, 38 GHz, and 60-GHz bands.

This work is related to the studies in [35] and [36]. In [34], separation distances of 8.2, 4.9, and 1 km are suggested for the 28 GHz, 38 GHz, and 60 GHz bands to reduce the interference below the noise level for the FS system from a 5G base station (BS). These distances are required when the FS station beam is directed toward the 5G BS. No interference is expected when the FS station is pointed in the opposite direction. The study assumed channel bandwidths of 200 MHz, 0.5 GHz, and 2.16 GHz for the 5G BS in the 28 GHz, 38 GHz and 60 GHz bands, respectively.

In the case where the FS BS is facing the opposite direction of the 5G UE, no interference is expected in the 38 GHz and 60 GHz bands, but a separation distance of 100 m is required for the 28 GHz band. In the case where the FS BS beam faces the 5G UE, separation distances of at least 8.6, 5.5, and 0.8 km are required for the 28 GHz, 38 GHz, and 60 GHz bands. It is observed that there is a possibility of co-existence between the two systems when there are specific distances between the 5G and FS systems. However, these studies did not address the 5G SEM as an interferer.

IV. A-MCL SPECTRUM-SHARING MODEL

The proposed model consists of two calculation parts: the interference and noise levels, in order to compute the interference-to-noise ratio (INR), which is a parameter on

which the terrestrial BS of the victim receiver relies to operate without harmful interference [37]. The interference level at the victim receiver can be calculated on the basis of the interferer parameters such as the power, antenna height, and gain; the victim antenna height gains; and the path loss based on the deployed environment. Finally, the PSD overlap loss is included in the interference calculation to represent the PSD overlap. In the following section, the steps for calculating the INR and a derivation of the PSD overlap loss from current studies are presented, followed by the proposed simplifications and modifications to the existing model.

A. INR SPECTRUM-SHARING CALCULATION

To ensure the protection of the primary service, the interfering signal should not exceed a certain threshold determined by the victim receiver. The general interference power received by the victim receiver, I (dBm), can be expressed as

$$I = P_{It} + G_{It} + G_{Vr} - L(f, d, Envir) + L_{PSDO}(f) - BW_{Corr}, \quad (1)$$

where P_{It} is the transmitter power of the interferer (dBm); G_{ti} and G_{rv} (dBi) are the antenna gains of the interfering transmitter and victim receiver, respectively; and L_{PSDO} (dB) is the interfering power attenuation loss due to the overlapping PSDs of the interfering transmitter and victim receiver.

The bandwidth difference between the interfering bandwidth BW_I and the victim bandwidth BW_V is represented by the bandwidth correlation factor $Band_{corr}$ (dB) as follows

$$Band_{corr} = \begin{cases} BW_I \geq BW_V & -10 * log\left(\dfrac{BW_I}{BW_V}\right). \\ BW_I < BW_V & 0 \end{cases} \quad (2)$$

The thermal noise of the victim receiver needs to be calculated in order to evaluate the INR level (dB). The noise floor N_p (dBm) is

$$N_p = -174 + 10log(BW_V) + N_f, \quad (3)$$

where N_f (dB) is the noise figure of the victim receiver.

Furthermore, the INR_{Target} for the 5G system and the FS is expressed as

$$INR_{Target} = \begin{cases} -6 \text{ dB } for \text{ 5G} \\ -10 \text{dB } for \text{ FS}. \end{cases} \quad (4)$$

INR_{Target} is the margin between the allowed interference and the victim receiver noise level. This means that the interference level should be lower than the 5G receiver noise level of 6 dB based on ITU reports [38], [39]. Similarly, the interference level should be 10 dB lower than the FS receiver noise level based on the ITU recommendation in [40]. These values will ensure co-existence in any compatibility study that is related to the 5G system or the FS system.

The spectrum-sharing criteria for both system in order to coexist can be defined as

$$INR_{Cal} \geq INR_{Target}. \quad (5)$$

The above equation shows that, in order to achieve co-existence for a specific sharing scenario, the calculated INR level (INR_{Cal}) should be equal to or greater than the target INR level. In fact, INR_{Cal} (dB) is calculated as follows

$$INR_{Cal} = I - N_P. \qquad (6)$$

In this section, the general equation of the PSD overlap when the 5G system acts as an interferer is introduced at the beginning. This will be followed by a derivation of the PSD in current studies, followed by the proposed simplifications to the current model. Finally, the PSD overlap when the FS system acts as an interferer is derived.

The L_{PSDO} is derived by analyzing the overlap of the PSDs of the victim and interferer, as shown in Fig. 3. On the basis of the PSD of the interferer and the bandwidth of the victim receiver, the calculation of the PSD overlap loss will be derived in the following sections.
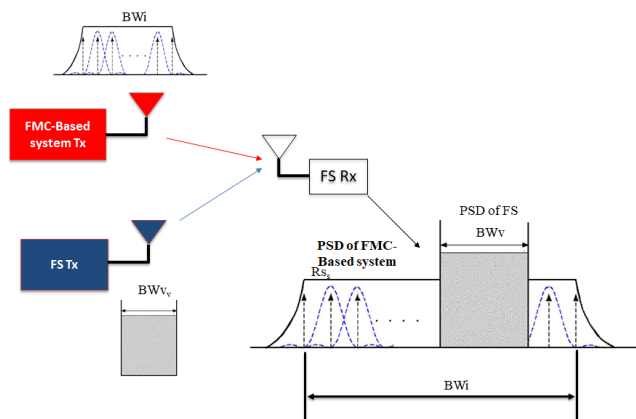
FIGURE 3. Overlap of the PSDs of an OFDM-based system and FS system when both systems are in the transmission (Tx) or receiving (Rx) mode.

As mentioned in Section II-C, this study considers the 5G system represented by an OFDM waveform. Furthermore, this study assumes that the system has N subcarriers with a rectangular pulse shape in the time domain and *sinc* in the frequency domain; as a result, the PSD of the signal is [4]

$$S_{5G}(f) = \sum_{i=0}^{N-1} \frac{P_{5G}}{R_{5G}} sinc^2 \left(\frac{f}{R_{5G}} - i \right), \qquad (7)$$

where P_{5G} is the power of the *i*th OFDM subcarrier and R_{5G} is the subcarrier spacing. This study assumes that $P_{s,5G}$ is equal to the total transmit power over the number of subcarriers, i.e., $P_{I,5G}/N$.

The PSD of the FS system S_{Fs} is a rectangular function in frequency domain and expressed as [4]:

$$S_{Fs}(f) = \frac{P_{FS}}{W_{FS}} rect \left(\frac{f}{W_{FS}} \right), \qquad (8)$$

where P_{FS} is the FS transmit power [41].

The general equation for the power attenuation due to L_P between the interfering transmitter and the victim receiver is

$$L_P = 10\log_{10} \left(\frac{\int_{f-BW_v/2}^{f+BW_v/2} S_{It}(f)\,df}{P_I} \right). \qquad (9)$$

1) PSD OVERLAP WHEN THE 5G SYSTEM ACTS AS AN INTERFERER

In the following section, the derivation of the PSD that was conducted in [4]–[6] and [10] is presented. This presentation is included in this study to present the common equations between the proposed simplification and the existing model and to show where the proposed simplification starts and what was simplified from the existing model.

a: Derivation of the PSD Overlap Attenuation in the Current A-MCL Model [4]–[6], [10]

The PSD overlap loss when the 5G system is an interferer to the FS is represented by L_{PSDO5G}. $S_{5G}(f)$ in (7) will be integrated between $f + \frac{W_{FS}}{2}$ and $f - \frac{W_{FS}}{2}$ of the FS bandwidth, as shown in Fig. 3. Therefore, L_{5G} is calculated as

$$L_{5G} = 10\log_{10} \left(\frac{\int_{f-W_{FS}/2}^{f+W_{FS}/2} \sum_{i=0}^{N-1} \frac{P_{5G}}{R_{5G}} \text{sinc}^2 \left(\frac{f}{R_{5G}} - i \right) df}{PI_{5G}} \right). \qquad (10)$$

The integral in the numerator is sloved first. Since $\text{sinc}^2(x) = \frac{\sin^2(\pi x)}{(\pi x)^2}$, (10) becomes

$$\int_{f-W_{FS}/2}^{f+W_{FS}/2} \sum_{i=0}^{N-1} \frac{P_{5G}}{R_{5G}} \left(\frac{\sin^2 \left\{ \pi \left(\frac{f}{R_{5G}} - i \right) \right\}}{\left(\pi \left(\frac{f}{R_{5G}} - i \right) \right)^2} \right) df. \qquad (11)$$

By assuming that $a = \frac{f}{R_{5G}} + \frac{W_{FS}}{2R_{5G}}$, $b = \frac{f}{R_{5G}} - \frac{W_{FS}}{2R_{5G}}$, and $X = \pi \left(\frac{f}{R_{5G}} - i \right)$ in (11) and by differentiatting both sides $df = \left(\frac{R_{5G}}{\pi} dx \right)$, (11) becomes

$$\frac{P_{S5G}}{\pi} \sum_{i=0}^{N-1} \int_{\pi(b-i)}^{\pi(a-i)} \left(\frac{\sin^2(x)}{x^2} \right) dx. \qquad (12)$$

Since $\sin^2(x) = \frac{1}{2}(1 - \cos(2x))$ [43], (12) becomes

$$\frac{P_{5G}}{2\pi} \sum_{i=0}^{N-1} \int_{\pi(b-i)}^{\pi(a-i)} \left\{ \left(\frac{1}{x^2} \right) - \left(\frac{\cos(2x)}{x^2} \right) \right\} dx. \qquad (13)$$

The solution of the first term of the integral in (13) is $\frac{1}{\pi(b-i)} - \frac{1}{\pi(a-i)}$. For the second term, using the information in [43], it is found that

$$\int_{\pi(b-i)}^{\pi(a-i)} \left(\frac{\cos(2x)}{x^2} \right)$$
$$= \frac{\cos\pi\,[2\,(b-i)]}{\pi\,[2\,(b-i)]} - \frac{\cos\pi\,[2\,(a-i)]}{\pi\,[2\,(a-i)]} - \int_{\pi(b-i)}^{\pi(a-i)} \frac{\sin(2x)}{x} dx.$$

By using a Taylor series, $sin(2x)$ can be written as

$$sin(2x) = \sum_{n=1}^{\infty} \frac{(-1)^n}{(2n+1)!}(2x)^{2n+1}. \tag{14}$$

Thus, the integral of the second term in (13) becomes $\int_{\pi(b-i)}^{\pi(a-i)} \frac{sin(2x)}{x}dx = \sum_{n=1}^{\infty} \frac{(-1)^n}{(2n+1)!}\int_{\pi(b-i)}^{\pi(a-i)}(2x)^{2n+1}dx$ and

$$\int_{\pi(b-i)}^{\pi(a-i)} \frac{sin(2x)}{x}dx$$
$$= 2\sum_{n=1}^{\infty} \frac{(-1)^n}{(2n+1)!}\left[(a-i)^{2n+1}-(b-i)^{2n+1}\right]. \tag{15}$$

By substituting (14) and (15) into (13), L_{PSDO5G} in (10) can be written as

Equation (16), as shown at the top of the next page, is the PSD overlap loss when the 5G system interferes with the FS system. This PSD overlap incorporates the bandwidth correlation factor. Thus, the general equation (1) can be rewritten as:

$$I_{Vr \to It} = P_{It} + G_{It} + G_{VR} - L(f, d, Envir) + L_{PSDO}(f). $$

2) SIMPLIFIED FORMULA OF THE A-MCL MODEL

We start our derivation from (10). We assume that $y = \left(\frac{f}{R_{5G}}-i\right)$. By utilizing the $\int u.dv = u.v - \int v.du$ integration method and assuming that $u = sin^2(y)$ and $dv = \frac{1}{y^2}dy$, we obtain the following

$$\int_{\pi(b-i)}^{\pi(a-i)} u.dv$$
$$= \frac{sin^2\pi(b-i)}{\pi(b-i)} - \frac{sin^2\pi(a-i)}{\pi(a-i)} + 2\int_{\pi(b-i)}^{\pi(a-i)} \frac{sin(y)cos(y)}{y}dy.$$

The integral of the second term is

$$\int_{\pi(b-i)}^{\pi(a-i)} \frac{sin(y)cos(y)}{y}dy = Si(\pi(a-i)) - Si(\pi(b-i)), \tag{17}$$

where $Si(y)$ is the sine integral function expressed as $\int_0^t \frac{sin(y)}{y}dy$, as shown in [43]. L_{PSDO5G} (dB) is then expressed as

$$L_{P5G} = 10log_{10}\left(\frac{P_{5G}\sum_{i=0}^{N-1}\left\{\begin{array}{c}Si\{\pi(a-i)-\\Si(\pi(b-i)\}\\+\left[\begin{array}{c}\frac{sin^2\pi(b-i)}{\pi(b-i)}-\\\frac{sin^2\pi(a-i)}{\pi(a-i)}\end{array}\right]\end{array}\right\}}{P_{I,5G}}\right). \tag{18}$$

3) PSD OVERLAP WHEN THE FS ACTS AS AN INTERFERER

In this case, the FS system acts as an interferer for the 5G victim receiver. The PSD of the FS is presented in (8), which is the function that expresses the interference with the PSD of the 5G system. The power loss due to L_{FS} is expressed as:

$$L_{FS} = 10log_{10}\left(\frac{\frac{P_{I,FS}}{W_{FS}}\int_b^a rect\left(\frac{f}{W_{FS}}\right)df}{P_{FS}}\right). \tag{19}$$

The solution of (19) is obtained by integrating the rectangle function between $a = \frac{f+\frac{W_{5G}}{2}}{W_{FS}}$ and $b = \frac{f-\frac{W_{5G}}{2}}{W_{FS}}$ when the 5G band fully covers the FS band. The result for L_{PSDOFS} (dB) is

$$L_{PSDOFS} = \begin{cases} 10log_{10}\left(\frac{W_{5G}}{W_{FS}}\right) & W_{5G} < W_{FS} \\ 10log_{10}\left(\frac{W_{FS}}{W_{FS}}\right) = 0 & W_{5G} \geq W_{FS}. \end{cases} \tag{20}$$

The above results show that the PSD overlap will always be equal to zero because the 5G bandwidth is larger than the FS bandwidth.

4) PROPAGATION MODELS AND ITU-R P.452-16 MODEL

The ITU-R P.452-16 propagation model is suitable for representing the 5G BS and FS BS pathloss and has been used in different ITU sharing studies [44]–[48]. The frequency range is 0.1–50 GHz [49]. The distance covered is up to 10000 km.

The pathloss PL (dB) is calculated as [49]

$$PL = 92.5 + 20log(f) + 20log(d) + CL, \tag{21}$$

where CL (dB) is the clutter loss expressed as

$$CL = 10.25 \times F_c$$
$$\times e^{-d_K}\left\{1-tanh\left[6\times\left(\frac{h}{h_a}-0.625\right)\right]\right\}-0.003, \tag{22}$$

where d_k (km) is the distance between the nominal clutter point and the antenna of the receiver, h (m) is the antenna height of the receiver above the ground, and h_a (m) is the nominal clutter height above the ground. Finally, the nominal factor F_c can be calculated as

$$F_C = 0.25 + 0.375 \times [1+tanh(0.75 \times (F_C - 0.5)], \tag{23}$$

where F_c is the operating frequency (GHz). The value of d_k is 0.002 km for urban areas, and h_a is 20 m for urban areas.

B. ANTENNA PATTERN
1) IMT-2020
The studies in [50] and [51] provide information regarding antenna modeling for the IMT-2020 system. In this section, the antenna pattern equations that are used in those studies is presented. The 3D beamforming radiation is composed of the vertical radiation pattern $A_{E,V}$ at the elevation angle θ and

$$L_{5G} = 10\log_{10}\left(\frac{P_{5G}\sum_{i=0}^{N-1}\left\{\begin{array}{c}\frac{1}{\pi(a-i)} - \frac{1}{\pi(b-i)} - \\ \left[\begin{array}{c}\frac{\cos\pi[2(b-i)]}{\pi[2(b-i)]} \\ -\frac{\cos\pi[2(a-i)]}{\pi[2(a-i)]}\end{array}\right] \\ -\left[\begin{array}{c}2\sum_{n=1}^{\infty}\frac{(-1)^n}{(2n+1)!} \\ \left[(a-i)^{2n+1} - (b-i)^{2n+1}\right]\end{array}\right]\end{array}\right\}}{2\pi P_{I5G}}\right). \tag{16}$$

the horizontal radiation pattern $A_{E,H}$ at the azimuth angle φ, which are expressed as follows [47], [48]

$$A_{E,V}(\theta) = -min\left\{12\left(\frac{\theta - 90°}{\theta_{3dB}}\right)^2, SLA_V\right\}, \tag{24}$$

$$A_{E,H}(\varphi) = -min\left\{12\left(\frac{\varphi}{\varphi_{3dB}}\right)^2, A_m\right\}, \tag{25}$$

$$A_E(\theta, \varphi) = G_{E,max} - min\left\{-\left[A_{E,V}(\theta) + A_{E,H}(\varphi)\right], A_m\right\}, \tag{26}$$

where A_m is the front back ratio with a value of 30 dB, θ_{3B} is the vertical 3-dB beam with a value of 65°, and $\varphi \in [0^0, 180^0]$. The side lobe level limit (SLA_V) is 30 dB, φ_{3B} is the horizontal 3-dB beam with a value of 65°, and $\varphi \in [-180^0, 180^0]$. The antenna element pattern $A_E(\theta, \varphi)$

(dB) is shown in Fig. 4. The side lobe level limit (SLA_V) is 30 dB, φ_{3B}

The combination of these two antenna parameters will result in $A_{c,i}$ for beam i, which is expressed as [52]

$$A_{c,i} = G_{E,max} - min\left\{-\left[A_{E,V}(\theta) + A_{E,H}(\varphi)\right], A_m\right\} + 10\log\left(\left|\sum_{m=1}^{N_H}\sum_{n=1}^{N_V}w_{i,m,n}.v_{m,n}\right|\right). \tag{27}$$

$v_{m,n}$ is the steering matrix component and also known as the superposition vector given by

$$v_{m,n} = e^{\left(\sqrt{-1}.2\pi\left((n-1).\frac{d_V}{\lambda}\cos(\theta) + (m-1).\frac{d_H}{\lambda}.\sin(\theta).\sin(\varphi)\right)\right)},$$

where n is the number of horizontal elements, which is equal to 1, 2, ..., N_V, and m is the number of vertical elements, which is equal to 1, 2, ..., N_H. N_V and N_H are the total
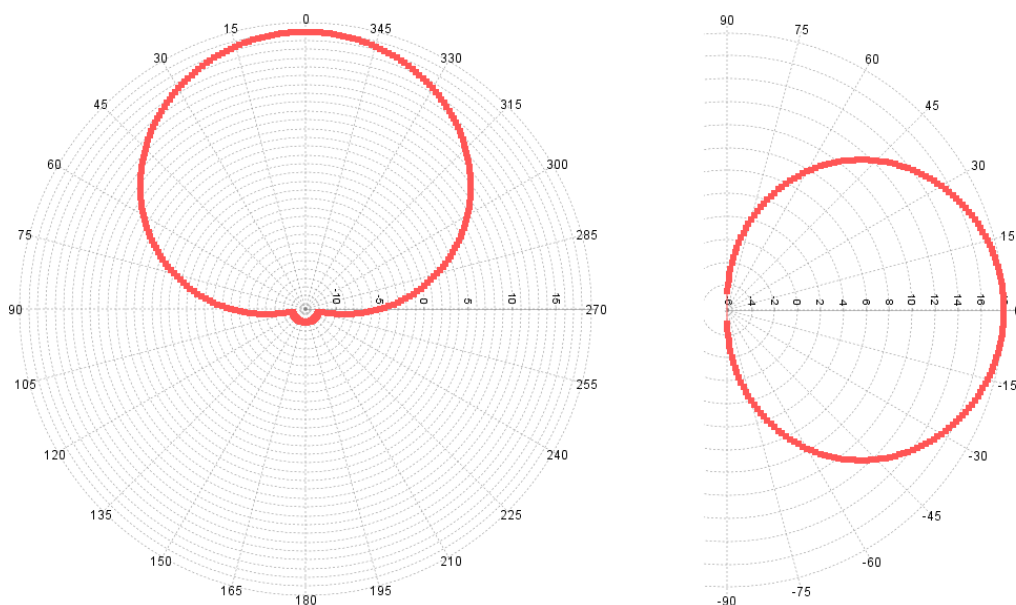

FIGURE 4. Vertical (left) and horizontal (right) element antenna patterns for the 5G system [49].
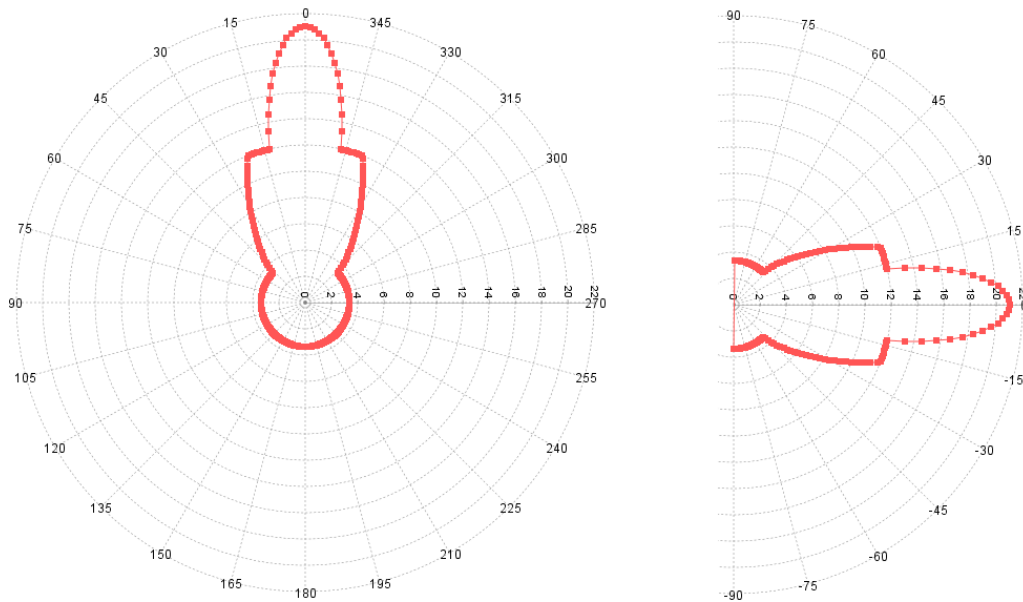
FIGURE 5. Vertical (left) and horizontal (right) antenna patterns for the FS system [53].

numbers of vertical and horizontal elements. $w_{i,m,n}$ is the weighting vector given by

$w_{i,m,n}$

$$= \frac{1}{\sqrt{N_H N_V}} e^{\left(\sqrt{-1}.2\pi \left(\begin{array}{c}(n-1).\frac{d_V}{\lambda}\sin\left(\theta_{i,etilt}\right)-(m-1).\\ \frac{d_H}{\lambda}.\cos\left(\theta_{i,etilt}\right).\sin\left(\varphi_{i,escan}\right)\end{array}\right)\right)},$$

where $\theta_{i,etilt}$ and $\varphi_{i,escan}$ are the electrical down-tilt steering and electrical horizontal steering, respectively.

Several antennas configurations are presented in [48]. For this study, the configuration A10 is selected as a balance between lowering the complexity of the simulation and having a sufficient number of antenna elements to represent the composite antennas. Configuration A10 has one column consisting of 10 antennas with a vertical spacing of 0.9λ. The total maximum gain is 18 dBi.

2) FIXED SERVICE

The latest version of the FS antenna model is detailed in ITU recommendation F.699-7 [53]. This recommendation presents the radiation pattern for the FS at operating frequencies between 100 MHz and 70 GHz. Several studies on sharing between the IMT and FS systems conducted by the ITU adopted this pattern [44]–[48]. The vertical and horizontal antenna patterns are shown in Fig. 5. For the frequency range of 1–70 GHz, the following equations are used

$$G(\varphi) = \begin{cases} G_{max} - 2.5 \times 10^{-3} \left(\frac{D}{\lambda}\varphi\right) & \text{for } 0° < \varphi < \varphi_m \\ = G_1 = 2 + 15\log\left(\frac{D}{\lambda}\right) & \text{for } \varphi_m < \varphi < \varphi_r \\ 32 - 25\log\varphi & \text{for } \varphi_r < \varphi < 48° \\ -10 - 10\log\left(\frac{D}{\lambda}\right) & \text{for } 48° < \varphi < 180°, \end{cases}$$
(28)

where G_{max} is the maximum antenna gain (dBi), D is the antenna diameter (m), G_1 is the first side lobe, and φ_m and φ_r (degrees) are as follows:

$$\varphi_m = \frac{20\lambda}{D}\sqrt{G_{max} - G_1} \text{ and } \varphi_r = 15.85\left(\frac{D}{\lambda}\right)^{-0.6}.$$

C. SYSTEM PARAMETERS AND SHARING SCENARIO
1) SYSTEM PARAMETERS
Table 5 lists the 5G and FS system parameters that are used in the simulation. In this study, its assumed that both systems will be an interfering transmitter or a victim receiver in a case study. The 5G parameters are based on the latest 3GPP technical report that investigates the channel models for mobile systems operating above 6 GHz [50]. On the other hand, the FS parameters are based on the Canadian FS standard in [21] and ITU recommendation F.758 [42].

2) DEPLOYMENT SCENARIO
Two case studies are investigated: the interference effects from the 5G system on the FS and vice versa. Each will be employed in UMi environments. For the OFDM-based system, four bandwidths are analyzed—125 MHz, 250 MHz, 500 MHz, and 1 GHz to reflect the effects of different bandwidths. Both systems will be employed in a co-channel sharing scenario. Fig. 6 shows the sharing scenario between both systems and that the analysis investigates the effect of the antenna position when the main beams of both systems face each other and when they are entirely opposite, which depends on the azimuth angle of the interferer φ_{It} and that of the victim φ_{Vr}.

TABLE 5. 5G and FS system parameters.

Parameter	5G BS		FS	
	Transmitter	Receiver	Transmitter	Receiver
Operating frequency f (GHz)	28.150 [21][55]			
Transmitted power Pt (dBm)	35 [22]	X	18 [40], [21]	X
Power of the subcarrier for the 5G system/In-band power for the FS system	Pt (mW)/N	X	30 dBm [39]	X
Modulation	QPSK [54]		QPSK [40]	
Multiplexing	OFDM		X	
Subcarrier frequency spacing R_S (kHz)	15 [54]		X	
Number of subcarriers N	BW/Rs [4]		X	
Bandwidth BW (MHz)	125, 250, 500, 1000 [12]		28 [21]	
BS gain G (dBi)	18 [50]	-12 [50]	21 [21]	
Noise figure N_f (dB)	X	9 dB [38], [54]	X	8 [40]
Antenna height h_t (m)	10 [49]	1.5 [49]	100 [21]	
Protection criteria INR (dB)	X	-6 [38], [39]	X	10 [40]
Antenna pattern	[50], [51], [21]		ITU-R F.699-8 [53]	
Environment supported	UMi LOS			
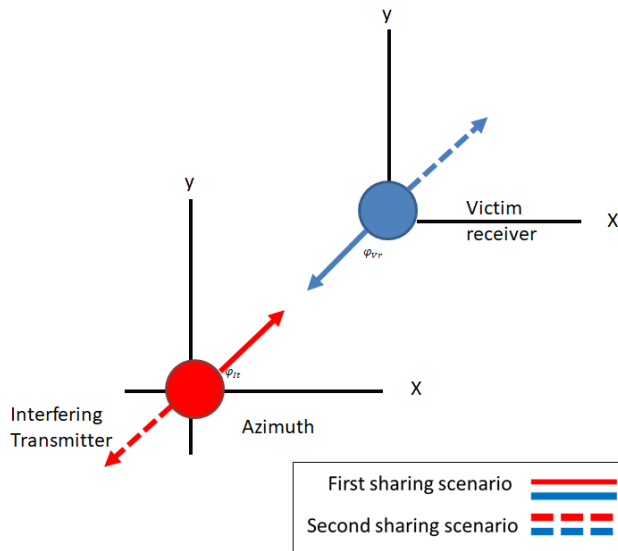
FIGURE 6. Sharing scenario when the main beams of both systems face each other.

FIGURE 7. Separation distances needed when the 5G system is interfering with the FS system (top) when both main beams face each other and (bottom) when both main beams are in opposite directions.

The co-located sharing scenario will also be investigated, where the antennas of the two services are placed in the same tower or too close to each other, and the distance (d) in kilometers approaches zero. This will show the possibility of sharing the same location.

V. RESULTS AND DISCUSSION

In this section, the results obtained for the deployment scenario are discussed and use the system parameters presented in Section IV. The intersection between the PSD overlap loss and INR_{Target} of the victim receiver (i.e., -6 dB for the 5G system and -10 dB for the FS) will result in the required separation distances.

A. 5G BS INTERFERING WITH THE FS VICTIM RECEIVER

Fig. 7 shows the required separation distances between the 5G interfering BS and the FS victim system in a UMi environment for four bandwidths. The top graph in Fig. 7 shows
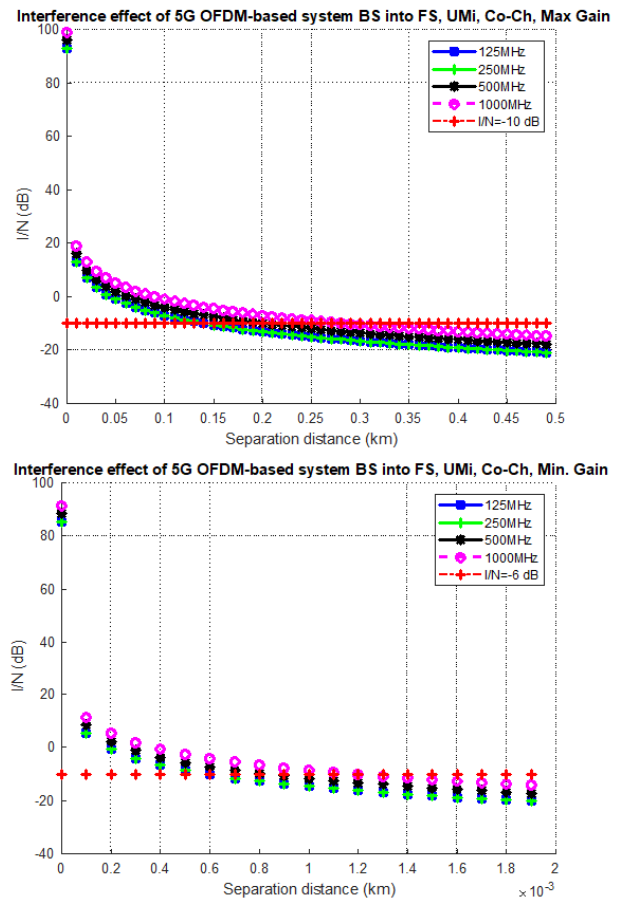
the interference effect when the main beams of both antennas face each other, whereas the bottom graph shows the results when both beams face away from each other.

The main outcomes from Fig. 7 are tabulated in Tables 6 and 7. Table 6 presents the results for the co-located sharing scenario. It is observed that both systems

TABLE 6. Colocation results when the 5G system is an interferer.

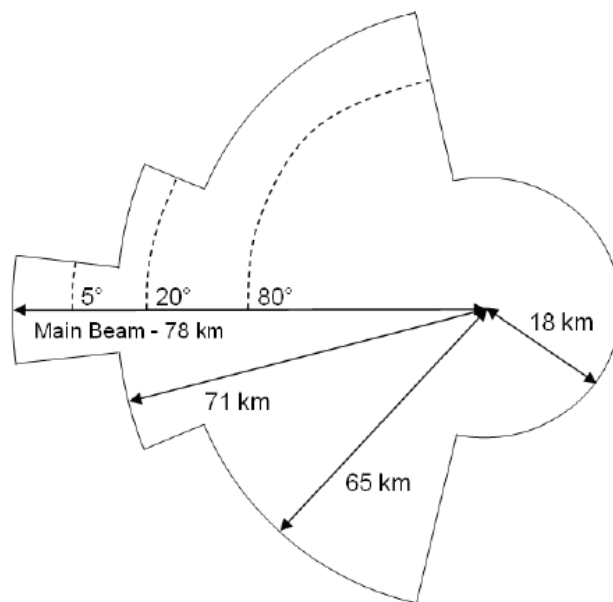| Bandwidth (MHz)	Co-located UMi (d ≈ 0) INR (dB)	
	Max. gain when the antennas point at each other	Min. gain when the antennas point opposite to each other
125	92.96	85.35
250	92.97	85.36
500	95.99	88.38
1000	99.03	91.42

TABLE 7. Required separation distances for the FS system to operate without harmful interference.

Bandwidth (MHz)	Separation Distance (km) UMi	
	Max. gain when the antennas point at each other	Min. gain when the antennas point opposite to each other
125	0.14	0.6×10^{-3}
250	0.14	0.6×10^{-3}
500	0.2	0.9×10^{-3}
1000	0.28	1.2×10^{-3}

cannot be co-located, even when both antenna beams face away from each other. The INR level is significantly high for different 5G bandwidths. For instance, an INR level of 85.35 dB is required when both antennas point in opposite directions, and the 5G system operates with a bandwidth of 125 MHz.

Table 7 lists the required separation distances when the 5G system acts as an interferer in the co-channel sharing scenario. The results show that a minimum distance of 0.14 km is required when the main beams of both systems face each other, and the 5G interfering BS bandwidth is 125 MHz. The distance increases as the 5G interfering bandwidth increases. For instance, for a 5G system bandwidth of 1 GHz, the required separation distance increases to 0.28 km, which results in a 100% increase in the separation distance when the 5G bandwidth increases from 0.125 GHz to 1 GHz (i.e., a 700% increase in the bandwidth).

In addition, the direction in which the antenna points plays a role in the reduction in the distance. When the main beams of both antennas point away from each other, the distances are reduced to 0.6 and 1.2 m for 5G bandwidths of 125 MHz and 1 GHz, respectively, which represents a reduction in the distance of 99.57% compared with the results when both antenna beams face each other. The results obtained are in agreement with the published results for the co-existence of the 5G and FS systems. In [34], a distance of 8.5 km between the mobile BS (with a bandwidth of 200 MHz) and the FS in the 28 GHz band is recommended. The achieved results are less than this owing to the use of the attenuated PSD overlap loss. From the above results, it can be seen that an increase in the bandwidth of the 5G victim increases the interference level at the FS victim receiver. This is due to the fact that in the 5G system, the number of subcarriers increases as the bandwidth increases, thus contributing to the interference level.

FIGURE 8. Coordination of the FS BS in the co-channel sharing scenario [21].

TABLE 8. Co-location results when the FS system is an interferer.

Bandwidth (MHz)	Co-located UMi (d ≈ 0) INR (dB)	
	Max. gain when the antennas point at each other	Min. gain when the antennas point opposite to each other
125	139.9	92
250	136.9	89.22
500	133.9	86.21
1000	130.8	83.2

TABLE 9. Required separation distances for the 5G system to operate without harmful interference.

Bandwidth (MHz)	Separation Distance (km) UMi	
	Max. gain when the antennas point at each other	Min. gain when the antennas point opposite to each other
125	20	82×10^{-3}
250	16	60×10^{-3}
500	10	41×10^{-3}
1000	7	30×10^{-3}

On the basis of the above results, the deployment of the 5G system is possible near the FS system when the appropriate distance is used. The co-channel coordination based on the Canadian specification for the FS is presented in [18], which states the required separation distances for co-channel coordination for different antenna radiation powers, as shown in Fig. 8.

In Fig. 8, it can be seen that for the main beam, a distance of 76 km is required, and a distance of 18 km is needed in the opposite direction of the main beam (i.e., the back lobe). On the basis of the obtained results and existing results, co-existence can be achieved since the obtained results show that lower distances than those mentioned in the recommendation for co-existence between two systems in the 28 GHz
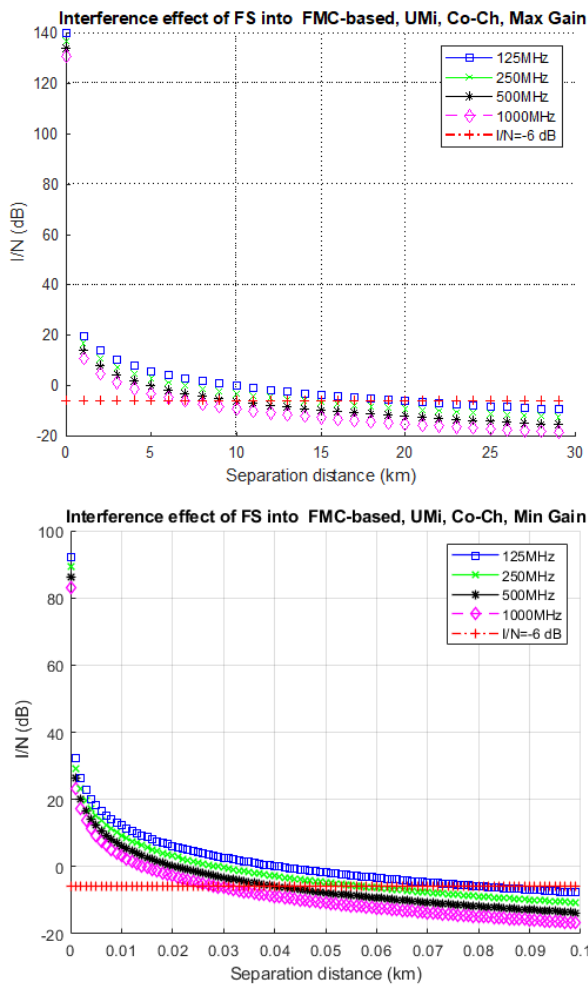
FIGURE 10. INR at the 5G victim receiver versus the 5G bandwidth.

FIGURE 9. INR at the 5G victim receiver versus the 5G bandwidth.

band are needed in the co-channel sharing scenario. In Fig. 8, it can be seen that for the main beam, a distance of 76 km is required, and a distance of 18 km is needed in the opposite direction of the main beam (i.e., the back lobe).

On the basis of this study results and existing results, co-existence can be achieved since the obtained results show that lower distances than those mentioned in the recommendation for co-existence between two systems in the 28 GHz band are needed in the co-channel sharing scenario the noise level increases as the bandwidth increases, as can be seen from (3), which makes the margin between the noise level and the interference level higher, as shown in Fig. 10.

The second outcome is that the required separation distances in this sharing scenario (i.e., the FS interfering with the 5G system) are larger than those of the previous sharing scenario (the 5G system interfering with the FS). This is due to the fact the PSD overlap loss in the case where the 5G system acts as the interferer is higher than that of when the FS acts as the interferer. The higher PSD overlap loss results in a lower INR level, leading to lower required separation distances to achieve co-existence. This indicates that the required separation distances when the FS acts as an interferer
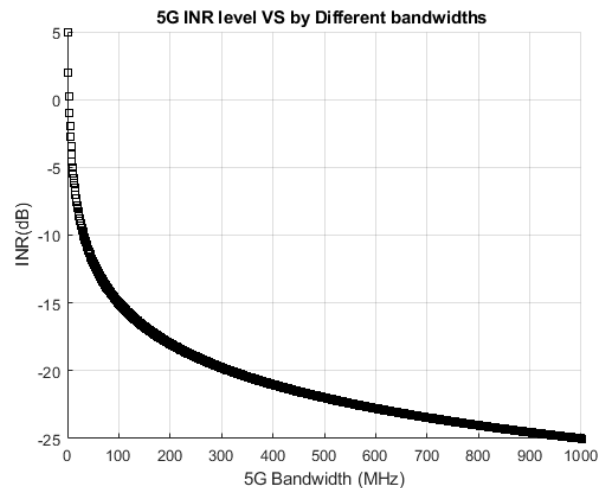
are larger than those when the 5G system is the interferer in this sharing scenario.

B. FS BS INTERFERING WITH THE 5G BS VICTIM RECEIVER

Similar to Fig. 7, the top and bottom graphs in Fig. 9 show the required separation distances for the operation of the 5G victim system when the interference level is 6 dB above the noise floor level. The graph in Fig. 9 shows the results when both antennas face each other, and also when they face in opposite directions.

The results for the co-located and co-channel sharing scenario are listed in Table 8. A very high INR is required in this sharing scenario; for instance, an INR level of 83.2 is produced when the bandwidth of the 5G victim receiver is 1 GHz and the main beams of both antennas face away from each other.

On the basis of Fig. 9, Table 9 summarizes the separation distances required for the 5G victim BS when the FS system acts as an interferer in the co-channel sharing scenario. In the case where both system antennas face each other, a distance of 20 km is required when the bandwidth of the 5G victim receiver is 125 MHz, which is reduced to 7 km for a bandwidth of 1 GHz. This translates to a 65% reduction in the distance when the bandwidth of the 5G victim receiver increases from 125 MHz to 1 GHz. In the case where the antennas face in opposite directions, a distance of 82 m is needed for the 5G system to operate with a bandwidth of 125 MHz, and the distance is reduced to 30 m when the bandwidth is 1 GHz. This translates to a 99.59% reduction in the distance compared with the results when both antenna beams face each other.

Two outcomes are obtained from the above results. First, the increase in the bandwidth of the 5G victim receiver reduces the INR level. This is due to the fact that the INR level is reduced as the bandwidth increases, as shown in Fig. 10.

In addition, the noise level increases as the bandwidth increases, as can be seen from (3), which makes the margin
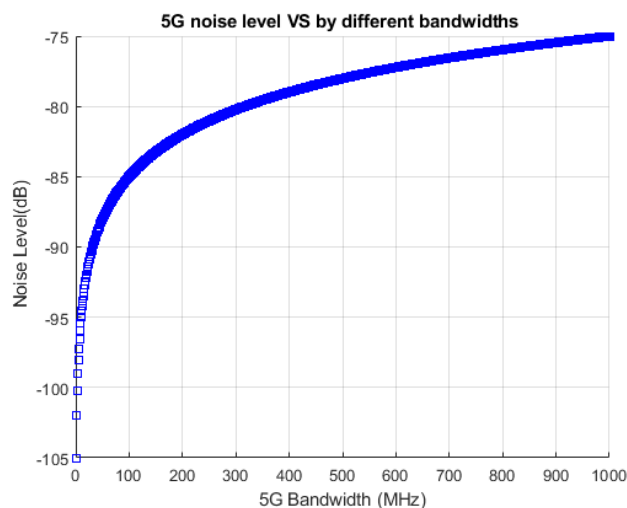
FIGURE 11. Noise level versus the 5G bandwidth.

between the noise level and the interference level higher, as shown in Fig. 11.

The second outcome is that the required separation distances in this sharing scenario (i.e., the FS interfering with the 5G system) are larger than those of the previous sharing scenario (the 5G system interfering with the FS). This difference in distances is due to the fact the PSD overlap loss in the case where the 5G system acts as the interferer is higher than that when the FS acts as the interferer. The higher PSD overlap loss results in a lower INR level, leading to lower required separation distances to achieve co-existence. This indicates that the required separation distances when the FS acts as an interferer are larger than those of the 5G system is the interferer in this sharing scenario.

VI. CONCLUSION

In this paper, the co-existence between a 5G system represented by an OFDM-based system and an FS system in the 28 GHz band based on Canadian frequency allocation and standards is presented. The current general mathematical model was utilized in a new application and modified by adding a 3D beamforming antenna for the 5G system to represent the PSD overlap loss between the interfering system and the victim receiver. The PSD overlap loss is helpful when the SEM of the interfering system is not available, which is the case in any newly introduced wireless system that needs spectrum-sharing studies before its deployment, e.g., the 5G system.

Two case studies were analyzed: first, the 5G system was assumed to interfere with the FS system. The results show that both systems cannot be co-located in the co-channel sharing scenario, even when both system antennas point in opposite directions. In the co-channel sharing scenario, co-existence is achieved when minimum separation distances of 0.14 and 0.28 km for 5G bandwidths of 125 MHz and 1 GHz, respectively, are applied. The distance increases by 100% when increasing the 5G bandwidth from 125 MHz to 1 GHz. These distances are reduced to 0.6 and 1.2 m when

both antennas point in opposite directions, translating to a reduction in the distance of nearly 99.57% due to antenna positioning. An increase in the 5G bandwidth will result in an increase in the INR level at the victim receiver, which means that a larger separation distance will be required.

Second, in the case where the FS system acts as the interferer, both systems cannot be co-located in the co-channel, even when both antennas point in opposite directions. Minimum separation distances of 20 and 7 km are needed when the 5G interfering BS bandwidths are 125 MHz and 1 GHz, respectively, and the main beams of both systems face each other to achieve co-existence. The increase in the 5G bandwidth contributes to a reduction in the distance of 65% (i.e., from 125 MHz to 1 GHz). The distances are reduced to 82 and 30 metres when both systems point away from each other and the 5G bandwidths are 0.5 and 1 GHz, respectively, which represent a 99.58% reduction in the distance.

On the basis of the Canadian requirements for FS system co-channel coordination, these results show the feasibility of co-existence between the 5G and FS system in the 28 GHz band when certain distances are applied and the antenna directions are appropriately set. This study contributes to worldwide efforts on spectrum-sharing studies as requested by the ITU. The proposed model can be used in the spectrum-sharing studies for future mobile generations such as 6G or the nth mobile generation before their official parameters are released, as long as the PSD is known.

REFERENCES

[1] *IMT-2020 Submission and Evaluation Process.* Accessed: Jan. 11, 2019. [Online]. Available: http://www.itu.int/en/ITU-R/study-groups/rsg5/rwp5d/imt-2020/Pages/submission-eval.aspx

[2] The International Wildlife Rehabilitation Council. (2015). *RESOLUTION 238 Studies on Frequency-Related Matters for International Mobile Telecommunications Identification Including Possible Additional Allocations to the Mobile Services on a Primary Basis in Portion(s) of the Frequency Range Between 24.25 and 86 GHz for the Future Development of International Mobile Telecommunications for 2020 and Beyond.* [Online]. Available: http://www.itu.int/dms_pub/itu-r/oth/0c/0a/R0C0A00000C0014PDFE.pdf

[3] "A comparison of the minimum coupling loss method, enhanced minimum coupling loss method, and the Monte-Carlo simulation CEPT," ERC, Brussels, Belgium, ERC Rep. 101, 1999. [Online]. Available: http://www.erodocdb.dk/docs/doc98/official/pdf/Rep101.pdf

[4] H.-S. Jo, H.-G. Yoon, J. Lim, W.-G. Chung, J.-G. Yook, and H.-K. Park, "The coexistence of OFDM-based systems beyond 3G with fixed service microwave systems," *J. Commun. Netw.*, vol. 8, no. 2, pp. 187–193, Jun. 2006.

[5] H.-S. Jo, H.-G. Yoon, J. Lim, and J.-G. Yook, "An advanced MCL method for assessing interference potential of OFDM-based systems beyond 3G with dynamic power allocation," in *Proc. Eur. Conf. Wireless Technol.*, Manchester, U.K., Sep. 2006, pp. 39–42.

[6] Z. A. Shamsan, T. A. Rahman, M. R. Kamarudin, A. M. Al-Hetar, and H.-S. Jo, "Coexistence of OFDM-based IMT-advanced and FM broadcasting systems," *Etri J.*, vol. 33, no. 2, pp. 279–282, Apr. 2011.

[7] Z. A. Shamsan, T. A. Rahman, and A. M. Al-Hetar, "Interference coordination for LTE-advanced and FM broadcasting interoperability," *Ann. Telecommun.*, vol. 67, nos. 9–10, pp. 477–483, Oct. 2012.

[8] Z. A. Shamsan, T. A. Rahman, and A. M. Al-Hetar, "Point-point fixed wireless and broadcasting services coexistence with IMT-Advanced system," *Prog. Electromagn. Res.*, vol. 122, pp. 537–555, Jan. 2012.

[9] Z. A. Shamsan and A. M. Al-Hetar, "An improved mathematical scheme for LTE-advanced coexistence with FM broadcasting service," *PLoS ONE*, vol. 11, no. 11, Nov. 2016, Art. no. e0136912.

[10] Z. A. Shamsan, "Bandwidth overlap factor for feasible coexistence of LTE-A and point to multipoint LMDS systems," *Wireless Pers. Commun.*, vol. 97, no. 2, pp. 2017–2035, Nov. 2017.

[11] 5G Americas. (Apr. 2017). *5G Spectrum Recommendations*. [Online]. Available: http://www.5gamericas.org/files/9114/9324/1786/5GA_5G_Spectrum_Recommendations_2017_FINAL.pdf

[12] S. A. Busari, S. Mumtaz, S. Al-Rubaye, and J. Rodriguez, "5G millimeter-wave mobile broadband: Performance and challenges," *IEEE Commun. Mag.*, vol. 56, no. 6, pp. 137–143, Jun. 2018.

[13] S. Yost. (Jun. 2016). *mmWave: Battle of the Bands*. [Online]. Available: http://www.comsoc.org/measuring-mmwave

[14] (Jun. 2017). *Consultation on Releasing Millimetre Wave Spectrum to Support 5G*. [Online]. Available: https://www.ic.gc.ca/eic/site/smt-gst.nsf/eng/sf11298.html

[15] Government of Canada. *What's New—2018*. Accessed: Mar. 19, 2019. [Online]. Available: https://www.ic.gc.ca/eic/site/smt-gst.nsf/eng/h_sf10780.html

[16] D. Paddon. (2016). *Canada to Hold Key 5G Spectrum Auction in 2020, Says Innovation Minister Bains*. [Online]. Available: https://www.cbc.ca/news/business/5g-wireless-spectrum-auction-1.4694214

[17] T. S. Rappaport, S. Sun, R. Mayzus, H. Zhao, Y. Azar, K. Wang, G. N. Wong, J. K. Schulz, M. Samimi, and F. Gutierrez, "Millimeter wave mobile communications for 5G cellular: It will work!" *IEEE Access*, vol. 1, pp. 335–349, 2013.

[18] Z. Qingling and J. Li, "Rain attenuation in millimeter wave ranges," in *Proc. 7th IEEE Int. Symp. Antennas, Propag. EM Theory*, Oct. 2006, pp. 1–4.

[19] *Frequency Allocations*, vol. 1, ITU Radio Regulations, Geneva, Switzerland, 2016.

[20] J. Chen, Z. Qian, T. Wang, and X. Li, "Analysis on the protection distance for spectrum sharing between IMT-2020(5G) and EESS systems in 25.5–27GHz band," in *Proc. IEEE 2nd Inf. Technol., Netw., Electron. Automat. Control Conf. (ITNEC)*, Dec. 2017, pp. 970–975.

[21] Industry Canada. (Sep. 2013). *SMSE-019-13 Technical Requirements for Fixed Radio Systems Operating in the Bands 25.25-26.5 GHz and 27.5-28.35 GHz*. [Online]. Available: https://www.ic.gc.ca/eic/site/smt-gst.nsf/eng/sf10684.html

[22] R. Stuhlfauth. (2016). *The Road to 5GLTE-A Evolution, Internet of Things and First 5G Aspects*. [Online]. Available: https://cdn.rohde-schwarz.com/fr/general_37/local_webpages/LTE-A_IoT_On-the_road_to_5G_RS_France_March2017_5G.pdf.

[23] P. Guan, D. Wu, T. Tian, J. Zhou, X. Zhang, L. Gu, A. Benjebbour, M. Iwabuchi, and Y. Kishiyama, "5G field trials: OFDM-based waveforms and mixed numerologies," *IEEE J. Sel. Areas Commun.*, vol. 35, no. 6, pp. 1234–1243, Jun. 2017.

[24] V. Vahidi and E. Saberinia, "OFDM high speed train communication systems in 5G cellular networks," in *Proc. 15th IEEE Annu. Consum. Commun. Netw. Conf. (CCNC)*, Jan. 2018, pp. 1–6.

[25] B. Farhang-Boroujeny and H. Moradi, "OFDM inspired waveforms for 5G," *IEEE Commun. Surveys Tuts.*, vol. 18, no. 4, pp. 2474–2492, 4th Quart., 2016.

[26] H. F. Arrano and C. A. Azurdia-Meza, "OFDM: Today and in the future of next generation wireless communications," in *Proc. IEEE Central Amer. Panama Student Conf. (CONESCAPAN)*, Sep. 2016, pp. 1–6.

[27] S. Sesia, I. Toufik, and M. Baker, *LTE—The UMTS Long Term Evolution: From Theory to Practice*. Hoboken, NJ, USA: Wiley, 2009.

[28] *Technical Feasibility of IMT in Bands Above 6 GHz*, Standard ITU-R M.2376-0, 2015. [Online]. Available: http://www.itu.int/pub/R-REP-M.2376

[29] *Base Station (BS) Radio Transmission and Reception (Release 15)*, document 3GPP TS 38.104 V15.2.0, 3GPP, 2018. [Online]. Available: https://portal.3gpp.org/desktopmodules/Specifications/SpecificationDetails.aspx?specificationId=3202

[30] W. G. Chung, H.-S. Jo, H.-G. Yoon, J.-W. Lim, J.-G. Yook, and H.-K. Park, "Advanced MCL method for sharing analysis of IMT-advanced systems," *Electron. Lett.*, vol. 42, no. 21, pp. 1234–1235, Oct. 2006.

[31] G. Hattab, E. Visotsky, M. Cudak, and A. Ghosh, "Coexistence of 5G mmWave users with incumbent fixed stations over 70 and 80 GHz," in *Proc. IEEE Globecom Workshops*, Dec. 2017, pp. 1–5.

[32] S. Kim, E. Visotsky, P. Moorut, K. Bechta, A. Ghosh, and C. Dietrich, "Coexistence of 5G with the incumbents in the 28 and 70 GHz bands," *IEEE J. Sel. Areas Commun.*, vol. 35, no. 6, pp. 1254–1268, Jun. 2017.

[33] M. Tercero, S. Sharma, M. Coldrey, and J. Kronander, "Coexistence between 5G and fixed services," in *Proc. IEEE 83rd Veh. Technol. Conf. (VTC Spring)*, May 2016, pp. 1–5.

[34] J. Kim, L. Xian, and A. S. Sadri, "Numerical simulation study for frequency sharing between micro-cellular systems and fixed service systems in millimeter-wave bands," *IEEE Access*, vol. 4, pp. 9847–9859, 2016.

[35] J. Kim, L. Xian, R. Arefi, and A. S. Sadri, "60 GHz frequency sharing study between fixed service systems and small-cell systems with modular antenna arrays," in *Proc. IEEE Globecom Workshops*, Dec. 2015, pp. 1–6.

[36] J. Kim, L. Xian, A. Maltsev, R. Arefi, and A. S. Sadri, "Study of coexistence between 5G small-cell systems and systems of the fixed service at 39 GHz band," in *IEEE MTT-S Int. Microw. Symp. Dig.*, May 2015, pp. 1–3.

[37] 201W. A. Hassan, H.-S. Jo, and A. R. Tharek, "The feasibility of coexistence between 5G and existing services in the IMT-2020 candidate bands in Malaysia," *IEEE Access*, vol. 5, pp. 14867–14888, 2017.

[38] *Characteristics of Terrestrial IMT-Advanced Systems for Frequency Sharing/Interference Analyses*, Standard ITU-R M.2292-0, 2013. [Online]. Available: https://www.itu.int/dms_pub/itu-r/opb/rep/R-REP-M.2292-2014-PDF-E.pdf

[39] *Compatibility Studies in Relation to Resolution 224 in the Bands 698-806 MHz and 790-862 MHz*, Standard ITU-R M.2241, 2011. [Online]. Available: http://www.itu.int/pub/R-REP-M.2241/

[40] *Point-to-multipoint systems in the fixed service*, Standard ITU-R F.755-2, 1999. [Online]. Available: https://www.itu.int/rec/R-REC-F.755-2-199905-I/en

[41] M. R. Spiegel and J. Liu, *Texts Mathematical Handbook of Formulas and Tables*. New York, NY, USA: McGraw-Hill, 1999.

[42] *System Parameters and Considerations in the Development of Criteria for Sharing or Compatibility Between Digital Fixed Wireless Systems in the Fixed Service and Systems in Other Services and Other Sources of Interference*, Standard ITU-R F.758-6, 2015. [Online]. Available: https://www.itu.int/rec/R-REC-F.758/en

[43] Mathworks. *Si: Sine Integral Function*. Accessed: Feb. 16, 2019. [Online]. Available: https://www.mathworks.com/help/symbolic/mupad_ref/si.html?searchHighlight=Si(x)&s_tid=doc_srchtitle

[44] *Sharing and compatibility Study Between International Mobile Telecommunication Systems and Point-to-Point Fixed Wireless Systems in the Frequency Band 4 400-4 990 MHz*, Standard ITU-R F.2327-0, 2014. [Online]. Available: http://www.itu.int/pub/R-REP-F.2327-2014

[45] *Sharing and Compatibility Study Between Indoor International Mobile Telecommunication Small Cells and Fixed Service Stations in the 5 925-6 425 MHz Frequency Band*, Standard ITU-R F.2326, 2014. [Online]. Available: http://www.itu.int/pub/R-REP-F.2326

[46] *Sharing and compatibility Between International Mobile Telecommunication Systems and Fixed Service Systems in the 3 400-4 200 MHz Frequency Range*, Standard ITU-R F.2328, 2014. [Online]. Available: https://www.itu.int/dms_pub/itu-r/opb/rep/R-REP-F.2328-2014-PDF-E.pdf

[47] *Sharing and Compatibility Between International Mobile Telecommunication Systems and Fixed Service Systems in the 470-694/698 MHz Frequency Range*, Standard ITU-R F.2331, 2014. [Online]. Available: http://www.itu.int/pub/R-REP-F.2331

[48] *Sharing and compatibility Study Between International Mobile Telecommunication and the Fixed Service in the Frequency Band 1 350-1 527 MHz*, Standard ITU-R F.2333, 2014. [Online]. Available: http://www.itu.int/pub/R-REP-F.2333

[49] *Prediction Procedure for the Evaluation of Interference Between Stations on the Surface of the Earth at Frequencies Above About 0.1 GHz*, Standard ITU-R P.452-16, 2015. [Online]. Available: https://www.itu.int/rec/R-REC-P.452/en

[50] *Study on Channel Model for Frequency Spectrum Above 6 GHz (Release 14)*, document 3GPP TR 38.901 V14.3.0, 3GPP, 2017. [Online]. Available: http://www.3gpp.org/DynaReport/38901.htm

[51] *Study of Radio ffrequency (RF) and Electromagnetic Compatibility (EMC) Requirements for Active Antenna Array System (AAS) Base Station*, document 3GPP TR 37.840 V12.1.0, 3GPP, 2013. [Online]. Available: https://portal.3gpp.org/desktopmodules/Specifications/SpecificationDetails.aspx?specificationId=2624

[52] *Modelling and Simulation of IMT Networks and Systems for use in Sharing and Compatibility Studies*, Standard ITU-R M.2101, 2017. [Online]. Available: https://www.itu.int/rec/R-REC-M.2101/en

[53] *Reference Radiation Patterns for Fixed Wireless System Antennas for use in Coordination Studies and Interference Assessment in the Frequency Range from 100 MHz to 70 GHz*, Standard ITU-R F.699-7, 2006. [Online]. Available: https://www.itu.int/rec/R-REC-F.699/en

[54] R. Schwarz. (2016). *6.2016-1MA271_0e. 5G Waveform Candidates.* [Online] Available: https://cdn.rohde-schwarz.com/pws/dl_downloads/ dl_application/application_notes/1ma271/1MA271_0e_5G_waveform_ candidates.pdf

[55] Government of Canada. (2018). *Canadian Table of Frequency Allocations.* [Online]. Available: https://www.ic.gc.ca/eic/site/smt-gst.nsf/eng/sf10759.html

WALID A. HASSAN (S'19–SM'13) was born in Basrah city in Iraq, in 1981. He received the B.Sc. degree from the Faculty of Electrical and Electronic Engineering (telecommunications major), Benghazi University (formerly Garyounis University), Libya, in 2006, the master's degree from the Faculty of Electrical Engineering, University Technology Malaysia, and the Ph.D. degree from the same university, in 2009 and 2012, respectively.

He is currently a Postdoctoral Fellow with Lakehead University in Thunderbay, ON, Canada. He was a Postdoctoral Fellow with the Universiti Technologi Malaysia. He is also the Director of the Basrah Wireless Communication Research Lab, Information and Communication Engineering Department, Basrah University College of Science and Technology, Iraq. He is the consular of the IEEE Basrah Student Branch. His research interests include frequency spectrum management, spectrum sharing methods, and cellular communication systems.

HAN-SHIN JO (S'06–M'10) received the B.S., M.S., and Ph.D. degrees in electrical and electronics engineering from Yonsei University, Seoul, Korea, in 2001, 2004, and 2009, respectively.

He is currently an Associate Professor with the Department of Electronics and Control Engineering, Hanbat National University, Daejeon, South Korea. He was a Postdoctoral Research Fellow with the Wireless Network and Communications Group, Department of Electrical and Computer Engineering, University of Texas at Austin, from 2009 to 2011. He developed Long Term Evolution (LTE) base stations at Samsung Electronics in 2011-2012. His current research interests include all aspects of MIMO (channel modeling, precoding, and scheduling with limited feedback, beamforming, SDMA, and massive MIMO), and applications of stochastic geometry and optimization theory to wireless cellular and ad hoc networks. He received the Samsung Electronics Graduate Fellowship in 2006-2008, the Korea Research Foundation BrainKorea21 Graduate Fellowship in 2006-2007, the Korea Research Foundation Postdoctoral Fellowship in 2009, and the ETRI Journal Best Paper Award in 2011.

SALAMA IKKI received the B.S. degree from Al-Isra University, Amman, Jordan, in 1996, the M.Sc. degree from the Arab Academy for Science and Technology and Maritime Transport, Alexandria, Egypt, in 2002, and the Ph.D. degree from the Memorial University of Newfoundland, St. Johns, in 2009, all in electrical engineering.

He was a Research Assistant with INRS, University of Quebec, Montreal, from 2010 to 2012, and a Post-Doctoral Fellow with the University of Waterloo, Waterloo, ON, Canada, from 2009 to 2010. He is currently an Associate Professor in wireless communications with the Department of Electrical Engineering, Lakehead University. He has been carrying out research in communications and signal processing for over 10 years. He is widely recognized as an expert in wireless communications. He has authored or coauthored over 100 papers in peer-reviewed IEEE international journals and conferences with over 3100 citations and has a current h-index of 28.

Dr. Ikki was a recipient of the Best Paper Award for the work published in the EURASIP Journal on Advances in Signal Processing and IEEE Communication Letters, the IEEE Wireless Communication Letters Exemplary Reviewer Certificate in 2012, and the Top Reviewer Certificate from IEEE Transactions on Vehicular Technology, in 2015. His Ph.D. student received second place for Best Poster from the School of Electrical and Electronic Engineering, Newcastle University, U.K., Annual Research Conference in 2014. He serves on the Editorial Board of the IEEE.

MAZIAR NEKOVEE is a Professor of Telecoms and Mobile Technologies and the Head of the Department of Engineering and Product Design with the University of Sussex, since February 2017. He also heads Advanced Communication, Mobile Technology, and IoT Research Centre at Sussex. He is (as the only U.K. academic) with the EU's 5G Infrastructure Association, where he advises the EC on 5G and beyond-5G Strategic Research Agenda. He is also on the steering board of the EPSRC-funded ComNet2 consortium in mobile technologies and the U.S. National Academy of Science (NSF) funded research coordination network on 5G communications and networks.

Prior to joining the University of Sussex, he was a Chief Engineer and the Head of 5G research with Samsung R&D, U.K., from 2013 to 2017, where he established, led, and greatly expanded Samsung's European and U.K. research operations in 5G infrastructure, with a focus on advanced technology development and IP generation (10 5G patents), contributions to 5G standards in 3GPP and industry collaborations and consensus building, as well as working closely with Samsung's Network Business in 5G. While at Samsung, he established and successfully led a large (19 partners) industry-led Horizon 2020 consortium (5G PPP mmMAGIC) which developed, channel models, access technologies, and architectural components of 5G mobile communication systems and standards operating in millimeter-wave frequencies (also known as 5G New Radio, 5G NR). From 2001 to 2013, he was with British Telcom (BT) Research and Technology, as Senior Scientist and subsequently a Team Leader. At BT, he carried and led the research in fixed and wireless communication technologies, including IP multicast, WiFi, IoT, cognitive radio, and social networks, as well as advising BT's business and strategy units on wireless technology and bidding strategy in 4G spectrum auction.

From 2006 to 2010, he also held a Royal Society (U.K. Academy of Science) 50% Industry Fellowship with the University College London (UCL), while at BT, developing novel platforms for parallel simulations of vehicular wireless communication networks, with applications in self-driving cars and intelligent transport systems. His Ph.D. and subsequent Post-docs with Imperial College focused on theory and first-principle calculations of electronic and optical properties of surfaces and interfaces using density functional theory, quantum Monte Carlo simulations, and massively parallel computing. He has authored over 100 peer-reviewed papers, one best-selling book "Cognitive Radio Communications and Networks: Principle and Practice" and has 13 patents in telecommunication and mobile technologies. He is a sought-after speaker at high level industry events, C-level meetings with European operators, policy makers, and international conferences. He is an Adviser to tech-funds and economists on telecom technology and ICT.